

Miniaturized Radio Repeater for Enhanced Wireless Connectivity of Ad-Hoc Networks

Young Jun Song, *Student Member, IEEE*, and Kamal Sarabandi, *Fellow, IEEE*

Abstract—A new concept for development of a high-gain and miniaturized radio repeater is presented in this paper. The proposed system utilizes a small array of low-profile miniaturized planar antennas with vertically polarized radiation pattern as well as a modified ring hybrid coupler as the array power distribution circuit and a low-power high-gain amplifier chain. In this configuration, a small receiving antenna is placed between a pair of transmit antenna array, which are fed 180° out of phase. The transmit array creates a null-plane where the receive antenna is placed, and this way an isolation value between the transmit and receive antennas in excess of 50 dB is achieved, while the shortest distance between the transmit and receive antennas is less than $0.16\lambda_0$. The proposed repeater has a small form factor and occupies a small volume ($0.22\lambda_0^2 \times 0.03\lambda_0$). A prototype of the miniaturized radio repeater is fabricated and measured to verify the system performance. A radar cross section of the repeater is measured for evaluating the overall system gain and its bandwidth. It is shown that an amplifier chain with a gain of 50 dB can be inserted between the transmit and receive antennas, which results in the measured repeater RCS of 21.3 dBsm.

Index Terms—Electromagnetic shielding, indoor radio communication, interference suppression, mutual coupling, repeaters.

I. INTRODUCTION

IN complex channel environments such as urban canyons and building interiors, the communication range is mainly restricted by the exorbitant path-loss between the two communication nodes. In indoor propagation scenarios, obstacles such as walls, ceilings, and furniture cause significant multiple reflections, scattering, and diffraction. In such environments, therefore, the communication inevitably depends on the multiple paths including reflections and diffractions. In the absence of line-of-sight (LOS) communication, the signal due to multi-path experiences fast fading, which can result in loss of connectivity, even over short distances [1] and [2]. Traditionally higher transmit power and closer communication nodes have been suggested for ad-hoc networks to improve the path-loss and overcome the adverse effects of the multi-path communication. However, such methods are power inefficient, require many nodes, lead to low data rate due to the higher latency, and

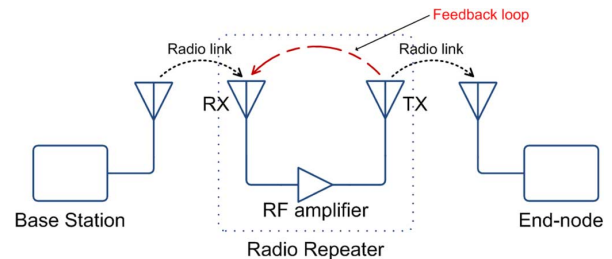


Fig. 1. Schematic of radio link using a radio repeater.

have the potential to cause unintended interference between neighboring nodes. In order to mitigate these problems and improve the wireless connectivity in complex environments, radio repeaters have been proposed as an alternative [3]–[8].

As shown in Fig. 1, a simple radio repeater can consist of receive antenna (RX), transmit antenna (TX), and an amplifier circuitry. The received signal from the base station in the line-of-sight is amplified and retransmitted to another repeater or the intended receive node that is in the line-of-sight. Unlike repeaters in transmission lines or optical fibers, the mutual coupling between the TX and RX antennas intrinsically restricts the performance and physical dimensions of the radio repeater. Because of the positive feedback loop between the TX and RX antennas (due to the radiation and near-field effects), the gain of the radio repeater is limited by this level of mutual coupling. To avoid this intrinsic problem, frequency-division duplex (FDD) and time-division duplex (TDD) have been extensively investigated, and some are reported in [9]–[11]. These strategies rely on suppression of the mutual coupling by choosing two different frequencies or separating the signal in time domain for the up and down links, respectively. However, these methods increase the system complexity, cost, and power consumption. Recently, a new concept for design of radio repeaters with a simple architecture was reported in [12]. This repeater utilizes two low-profile miniaturized antennas and a subwavelength metamaterial isolator to suppress the substrate modes and achieves an isolation in excess of 28 dB in a very small volume. As reported, the drawbacks of this repeater are low isolation and poor antenna efficiency. In a recent study, it was shown that the overall repeater gain (product of antenna and amplifier gains) of more than 35 dB is required for the repeater signal to overcome the multi-path signal in an indoor environment [13].

In this paper, a new concept for suppression of signal leakage between the TX and RX antennas is proposed and implemented. By utilizing a two-elements antenna array for the transmitter fed by a modified ring hybrid coupler, an electromagnetic null-plane is generated at the receiver location to reduce the mutual coupling drastically. The proposed radio repeater with a symmetric

Manuscript received December 15, 2011; accepted February 15, 2012. Date of publication May 23, 2012; date of current version July 31, 2012. This research was supported by the U.S. Army Research Laboratory under contract W911NF and prepared through collaborative participation in the Microelectronics Center of Micro Autonomous Systems and Technology (MAST) Collaborative Technology Alliance (CTA).

The authors are with the Radiation Laboratory, Department of Electrical Engineering and Computer Science, The University of Michigan at Ann Arbor, Ann Arbor, MI 48109-2122 USA (e-mail: yjsong@umich.edu; saraband@eecs.umich.edu).

Color versions of one or more of the figures in this paper are available online at <http://ieeexplore.ieee.org>.

Digital Object Identifier 10.1109/TAP.2012.2201124

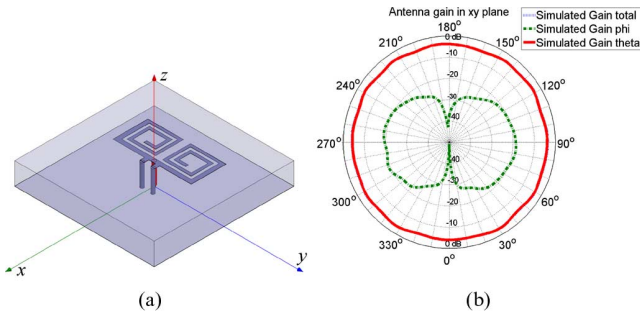


Fig. 2. Modified MMA: (a) geometry of the modified MMA and (b) simulated antenna gain in $H(xy)$ plane.

architecture is numerically analyzed, and its performance is experimentally verified. A prototype is fabricated using printed circuit technology on a commercially available dielectric substrate. The measurements show that the proposed repeater can boost the received signal by 50 dB and consequently has a radar cross section (RCS) value of 21.3 dBsm. This corresponds to the RCS of an equivalent metallic sphere having a diameter equal to 13.1 m. The proposed radio repeater utilizes miniaturized antennas capable of pure vertically polarized radiation pattern and 50-dB gain of cascaded RF amplifier. Antennas, RF circuitry, and dc power stage are fully integrated and packaged into a small size of 85.39 mm \times 39.67 mm \times 3.48 mm.

II. DESIGN SPECIFICATION FOR MINIATURIZED RADIO REPEATER

A. High-Gain Miniaturized Planar Antenna

It is well known that, for near-ground propagation scenarios, vertically polarized waves experience less path-loss than horizontally polarized waves [14]. For this purpose, radio repeaters considered here are equipped with antennas having vertical polarization while minimizing their height and lateral dimensions.

According to antenna theory, the gain of an antenna is proportional to its directivity and radiation efficiency. For small antennas, the antenna gain is mainly determined by the radiation efficiency, which relates to the conductor and dielectric losses. A low-profile miniaturized antenna with vertical polarization based on a quarter-wave microstrip resonator is reported in [12]. Although the reported multi-element monopole antenna (MMA) is capable of emanating omni-directional and vertical radiation pattern, its gain is limited by its poor radiation efficiency (about -9 dBi). Since the overall repeater system gain is proportional to the product of the TX and RX antenna gains, the antenna gain should be improved in the effort for increasing the repeater gain. One convenient way is to increase the height of the antenna. Because the vertical polarization mainly comes from the vertical current along the shorting pins, the antenna gain can be improved by simply extending the height of the shorting pins. However, it should be noted that the higher thickness of the substrate causes the stronger substrate modes, and consequently the higher mutual coupling between the antennas embedded in the same substrate. Increasing the height of the antenna from 1.57 mm (previous MMA design shown in Fig. 2 [12]) to 3.18 mm, the antenna gain is increased from -9 dBi to -4 dBi in the antenna H -plane. However, this value of gain is still too low and will degrade the overall repeater gain.

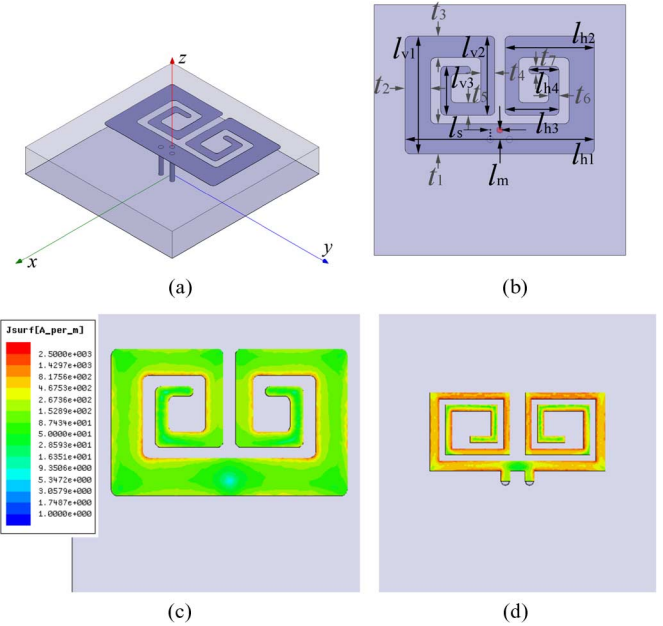


Fig. 3. Transmit antenna: (a) geometry of the TX; (b) design parameters; (c) simulated current distribution of the TX; and (d) simulated current distribution of the modified MMA.

Another idea for increasing the antenna gain and bandwidth is to reduce the stored electromagnetic energy and the conductor loss. These are mainly influenced by an electric current distribution over the metallic traces of the MMA. Due to shallow skin depth and fringing field effects at high frequency, the narrow width of the strips and the sharp edges at the corners contribute to the observed exorbitant ohmic loss. To alleviate the ohmic loss, the electric current must be distributed over wider strips, and the sharp edges be removed as shown in Fig. 3. As can be seen, the wide width of the metallic strips evenly distributes the electric current. In addition, the round corners minimize the current density and strong electric and magnetic fields around the corners. As a result, the overall intensity of the electric current over the traces is reduced down to 10% of the previous design. This reduction of the conducting loss and stored energy results in improvement of the antenna gain and bandwidth. As indicated in Fig. 4, the new miniaturized planar antenna shows good matching at the designed frequency and higher gain (-1 dBi) in the H -plane. This indicates that 6 dB of gain enhancement for the overall repeater system is achieved from the higher gain of the modified antennas. The physical design parameters are optimized for operation around 2.46 GHz and summarized in Table I.

B. Transmit-Receive Antenna Isolation

As mentioned before, the mutual coupling between the TX and RX antennas is the most critical factor that limits the maximum achievable repeater gain. Various approaches have been suggested and studied to suppress the mutual coupling in [15]–[12]. The mushroom type of metamaterial structure and electromagnetic band-gap (EBG) structure are commonly proposed and demonstrated in [15] and [16]. However, the metamaterial based approaches inevitably require periodic structures and consequently large physical dimensions. Although the magneto-dielectric embedded-circuit based method

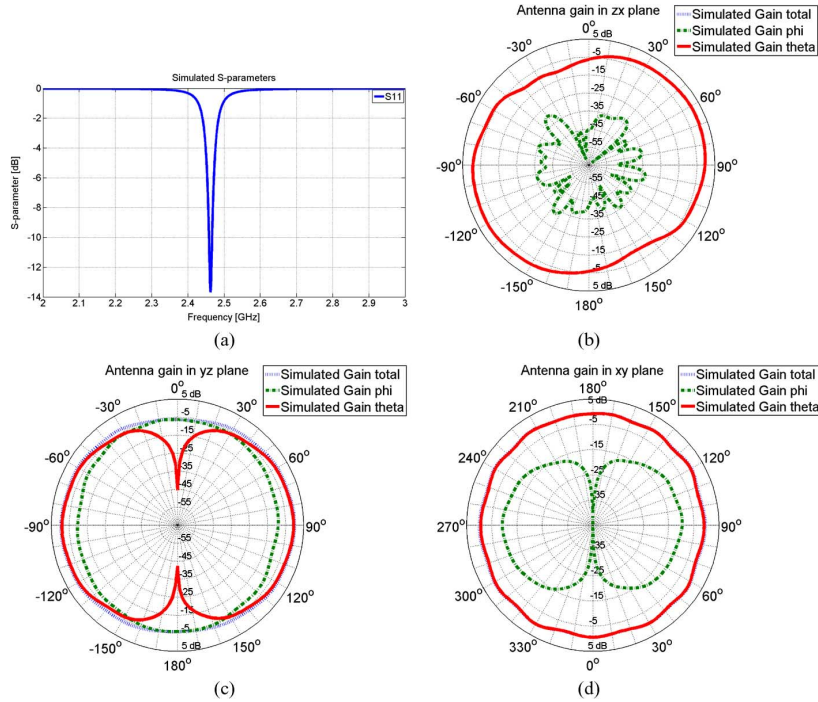


Fig. 4. Simulated responses of the TX: (a) S_{11} response; (b) radiation pattern in $E(zx)$ plane; (c) radiation pattern in $E(yz)$ plane; and (d) radiation pattern in $H(xy)$ plane.

TABLE I
DESIGN PARAMETERS OF THE REDESIGNED TRANSMIT ANTENNA

l_{h1}	l_{h2}	l_{h3}	l_{h4}	l_{v1}	l_{v2}
15.04 mm	7.11 mm	4.29 mm	2.39 mm	9.40 mm	6.30 mm
l_{v3}	l_m	l_s	t_1	t_2	t_3
3.89 mm	0.76 mm	0.76 mm	2.41 mm	2.01 mm	1.70 mm
	t_4	t_5	t_6	t_7	
	1.09 mm	0.99 mm	0.81 mm	0.61 mm	

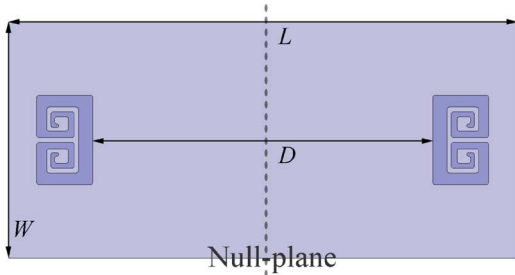


Fig. 5. Design parameters of the TX array.

in [18] can be adapted in a small system dimension, its coupling suppression is narrow-band and limited by the quality factor of the resonant EBG loops. With a finite Q factor, it was reported that the printed EBG structure can suppress the peak level of S_{21} from -18 dB to -28 dB in [12].

In order to achieve further suppression of the mutual coupling, a new concept based on generating a null-plane from a symmetric and out-of-phase pair of TX antennas is suggested. Feeding two antennas by signals having the same amplitude but 180° out of phase, the resulting electric field will vanish in the perpendicular bisect-plane of the substrate on which the antennas are built. As shown in Fig. 5, the TX antennas are positioned on the substrate in a symmetric manner.

If the receiver has a plane of symmetry that coincides with the perpendicular bisect-plane, the received voltage due to the mutual coupling will be zero. In this configuration, the null-plane exists independent of the separation between the two elements of the TX antenna array. However, if the two antennas are too close to each other, the transmit antenna gain will drop due to far-field cancellation. To avoid such cancellation in the far field, the TX antennas can be separated by $\lambda_0/2$ in which case the fields add up coherently in the far field in the end-fire directions. In these directions, the field is doubled, and the transmitter gain is increased by 6 dB. The antenna gain drops gradually as a function of angle towards the null-plane. To maximize the antenna gain, the distance D between the two TX antennas is set to 57.15 mm. The width W and length L of the substrate are optimized to 39.67 and 85.39 mm, respectively. The optimized TX array and its simulated radiation patterns are shown in Fig. 6. As expected, an electric null-plane is generated at the symmetric plane. It should be noted that since the power is split into two ways the overall repeater gain will be increased by 3 dB in the end-fire directions in the H -plane. As shown in Fig. 6(d), the half-power beamwidth of such array is very wide (more than 80° in each of the end-fire lobes).

C. Receive Antenna

The RX antenna should also operate with vertical polarization and have a plane of symmetry to be placed in the null-plane of the TX array. The antenna feed must be in the plane of symmetry and in the null-plane. This way, the retransmitted signal from the TX array will induce the electric currents in the opposite directions over the symmetric arms of the RX antenna. As a result, the induced current on the RX feed will be zero, and the desired isolation can be achieved. A topology similar to the TX antenna can be considered. To create a symmetric geometry, the topology of the TX antenna is imaged about its longer direction

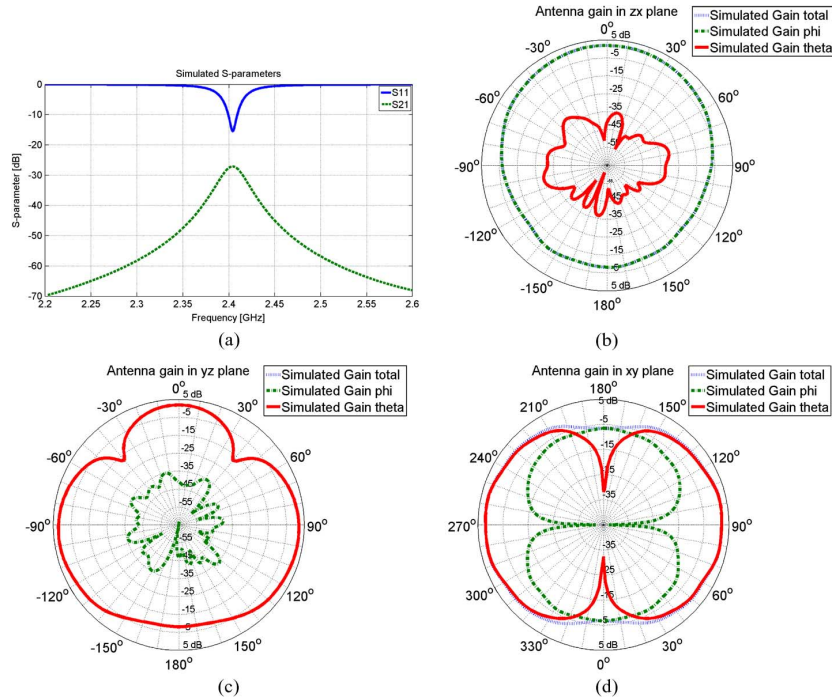


Fig. 6. Simulated responses of the TX array: (a) S_{11} response; (b) radiation pattern in $E(zx)$ plane; (c) radiation pattern in $E(yz)$ plane; and (d) radiation pattern in $H(xy)$ plane.

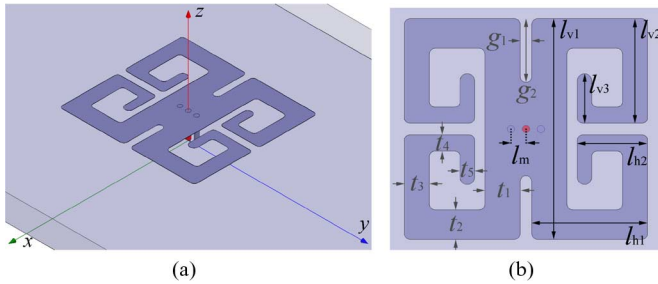


Fig. 7. Receive antenna: (a) geometry of the RX and (b) design parameters.

as shown in Fig. 7(a). However, the locations of the shorting pins and feed point are modified. Basically, the feed is placed in the plane of symmetry, and the shorting pins are also placed in a symmetric fashion with respect to the feeding pin and the plane of symmetry. This is shown more clearly in Fig. 7(b). In this figure, design parameters that influence the antenna characteristics, such as the resonant frequency, input impedance, bandwidth, and antenna efficiency, are also described.

Each arm of the 4-arm MMA is approximately a quarter wavelength long, which produces a strong electric current through the shorting pins. This, in turn, results in a purely vertical polarization radiation pattern. As the RX antenna occupies the larger volume and surface area, it shows the higher gain and bandwidth compared to the TX antenna. The input reflection coefficient and radiation patterns of the RX antenna are shown in Fig. 8. The numerically simulated vertical gain and bandwidth are shown to be -1.3 dBi in the H -plane and 15 MHz, respectively. The omni-directional and vertical polarization enables the repeater to receive the signal regardless of the location of the base station. The physical design parameters are optimized for operation around 2.41 GHz and summarized in Table II.

D. Modified Ring Hybrid Coupler

In Section II-B, the concept of repeater isolation based on the symmetric cancellation was described. In order to generate two signals with the same amplitude and 180° out of phase, a conventional ring hybrid coupler can be utilized. The ring hybrid coupler consists of sum and difference input ports and two output ports, as shown in [19]. By exciting only the difference input port and terminating the sum input port, two outputs can be produced with the same amplitude and 180° phase difference. To be integrated into the proposed radio repeater system with a limited space, the geometry of the conventional ring hybrid coupler is modified and optimized, as shown in Fig. 9(a). Since a cascaded RF amplifier is incorporated, any parasitic effects from its circuit layout should be considered in the design of the ring coupler as well. The modified ring hybrid coupler with sharp corners and an embedded circuit layout for the RF amplifier is designed and verified using a commercial finite element method solver (Ansoft's HFSS ver. 12.1). With some optimization, the physical parameters are designed so that the coupler can operate around the desired frequency (2.41 GHz). The design parameters are summarized in Table III. As can be seen in Fig. 9(b), the modified ring hybrid coupler produces two signals within 0.01 dB of variation in amplitude and less than 0.05° in phase. As indicated, the vector sum of two outputs shows extremely small value at the desired frequency of 2.41 GHz (-40 -dB bandwidth of 65 MHz).

III. NUMERICAL SIMULATION RESULTS

A. Full-Wave Simulation of Miniaturized Radio Repeater

In Section II, the specific design objective and the principle of operation were discussed. All of the subcomponents such as TX array, RX, ring hybrid coupler, and the circuit layout for the RF amplifier are integrated, as shown in Fig. 10(a). In order to take

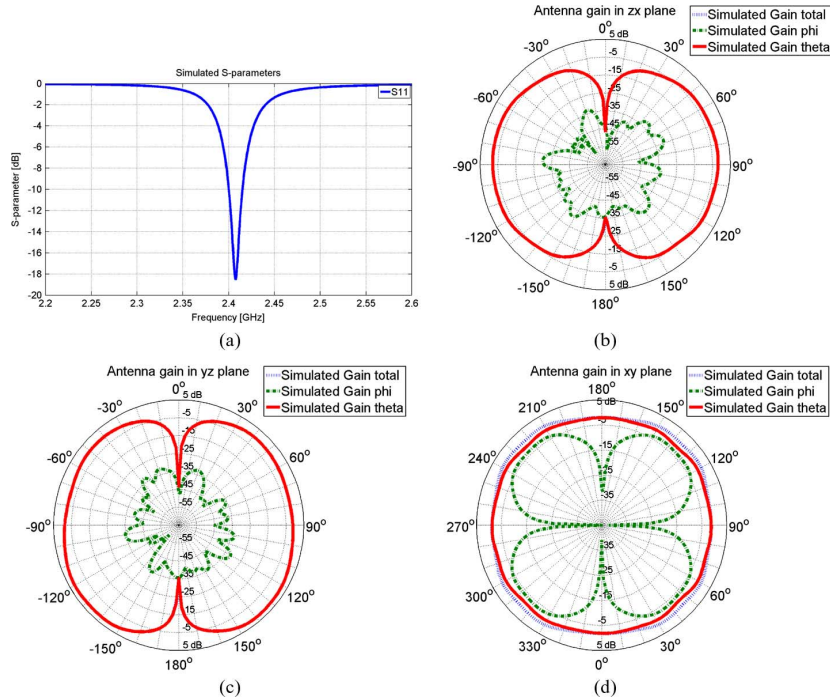


Fig. 8. Simulated responses of the RX: (a) S_{11} response; (b) radiation pattern in $E(zx)$ plane; (c) radiation pattern in $E(yz)$ plane; and (d) radiation pattern in $H(xy)$ plane.

any potential interactions between all subcomponents into account, the overall repeater system is further optimized and verified using Ansoft's HFSS. As shown in Fig. 10(b), the proposed symmetric cancellation method can suppress the mutual coupling between the TX and RX antennas down to -86 dB at the design frequency. Based on the bandwidth of the RF amplifier, the peak level of S_{21} should be considered to set the active gain of the proposed repeater. From the simulated responses, the RF amplifier is configured to 50 dB of gain.

Fig. 11 shows the magnitude of the electric near-field and far-field radiation patterns for the vertical polarization when the TX or RX antenna is separately excited. As expected, in TX mode, the near fields are perfectly symmetric, and the electric null-plane is generated along the symmetric plane in which the RX antenna resides. Furthermore, the far-field radiation pattern shows that the proposed radio repeater has wider beamwidth. In RX mode, the designed repeater shows a desired omni-directional radiation pattern.

B. Repeater Radar Cross Section

The repeater measurement of the overall system gain cannot be done using a network analyzer, as the connecting cables and the instrument can perturb the near fields and establish additional couplings between the TX and RX antennas. Also the antenna gains must be measured in the far field. Hence, the overall repeater gain must be characterized in a different fashion. The best way is through the measurement of the RCS of the repeater when the repeater is placed in isolation and the far-field region. The radio repeater can be viewed as a transponder, which can retransmit the received RF signal. The received RF signal by the radio repeater can be considered as an incident field and the retransmitted RF signal as a scattered field from the radio repeater. Thus, the RCS of the radio repeater can be easily calculated using Friis transmission formula.

Without loss of generality, suppose a monostatic radar utilized for the measurement of the repeater's RCS has an isotropic vertically polarized antenna and its output power is P_t . Then, the intensity of the received RF signal by the radio repeater can be expressed as

$$P_r = W_t A_{\text{eff}} = \frac{P_t}{4\pi R^2} A_{\text{eff}} \quad (1)$$

where W_t is the power density at the repeater, $A_{\text{eff}} = (\lambda_0^2/4\pi)G_r$ is the effective aperture of the repeater RX antenna, G_r is the gain of the repeater RX antenna, and R is the distance between the repeater and the radar. Since the repeater has an active gain G_{amp} , the power density of the retransmitted RF signal at the radar receiver is

$$W_s = \frac{P_s}{4\pi R^2} = \frac{P_r G_{\text{amp}} G_t}{4\pi R^2} \quad (2)$$

where P_s is the power intensity of the retransmitted RF signal by the repeater, and G_t is the gain of the repeater TX antenna. Hence, the radar cross section of the repeater is given by

$$\sigma_{\text{repeater}} = \lim_{R \rightarrow \infty} \left[4\pi R^2 \frac{W_s}{W_t} \right] = \frac{\lambda_0^2}{4\pi} G_r G_{\text{amp}} G_t \quad (3)$$

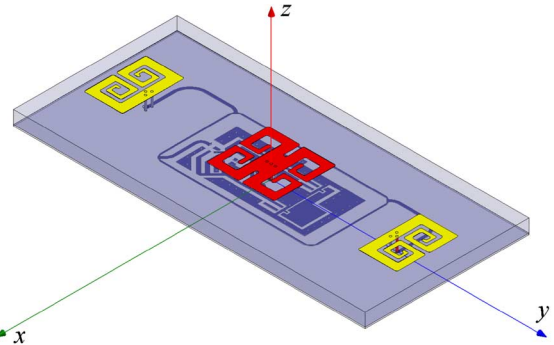
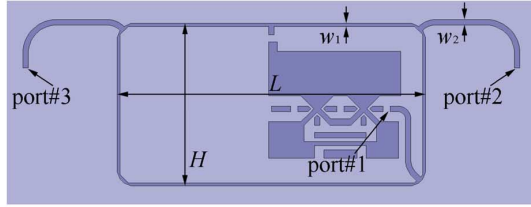
In order to calibrate the monostatic radar system, background subtraction method is performed, and a target with known RCS is measured and compared with the measured signal from the repeater. For this purpose, a 0.36-m-diameter metallic sphere is utilized. The approximate (assuming $a \gg \lambda_0$) RCS of a metallic sphere is given by

$$\sigma_{\text{sphere}} = \pi a^2 \quad (4)$$

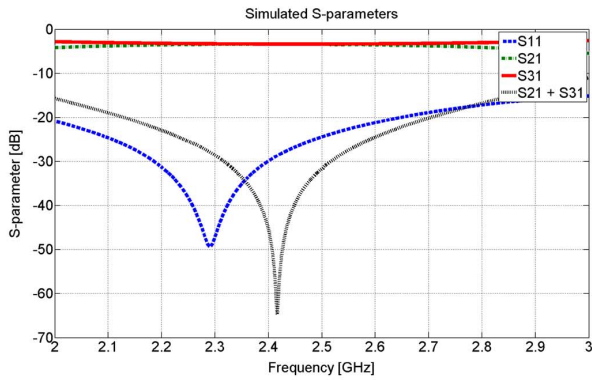
where a is the radius of the sphere. From (3) and (4), the diameter of an equivalent metallic sphere having the same RCS as the repeater also can be calculated.

TABLE II
DESIGN PARAMETERS OF THE REDESIGNED RECEIVE ANTENNA

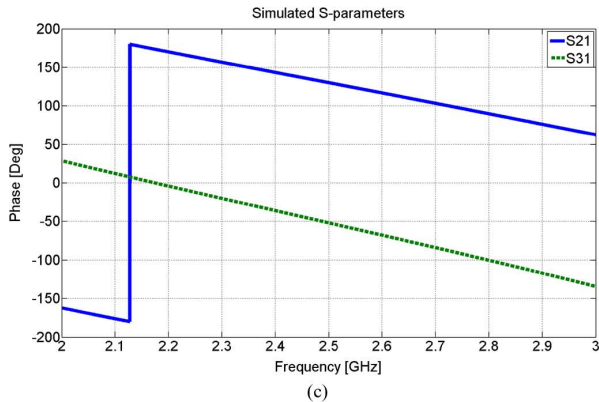
l_{h1}	l_{h2}	l_{v1}	l_{v2}	l_{v3}
7.87 mm	4.78 mm	15.04 mm	7.11 mm	3.37 mm
t_1	t_2	t_3	t_4	t_5
2.41 mm	2.01 mm	1.70 mm	1.09 mm	0.99 mm
	l_m	g_1	g_2	
	1.02 mm	0.76 mm	4.34 mm	



(a)



(b)



(c)

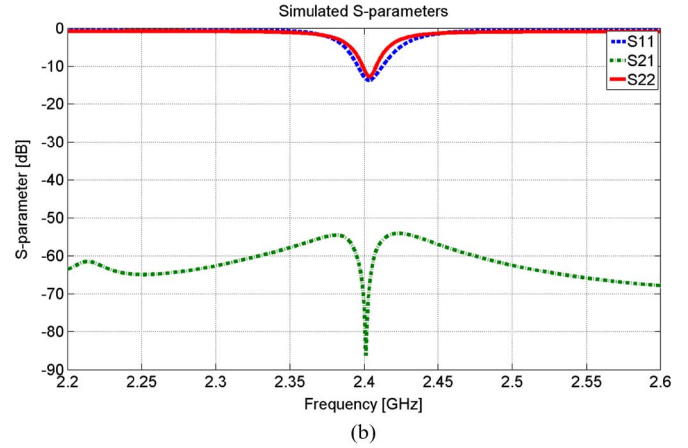
Fig. 9. Modified ring hybrid coupler: (a) geometry of the ring hybrid coupler; (b) simulated S-parameters; and (c) phase of two outputs.

TABLE III
DESIGN PARAMETERS OF THE MODIFIED RING HYBRID COUPLER

L	H	w_1	w_2
38.21 mm	20.14 mm	0.37 mm	0.68 mm

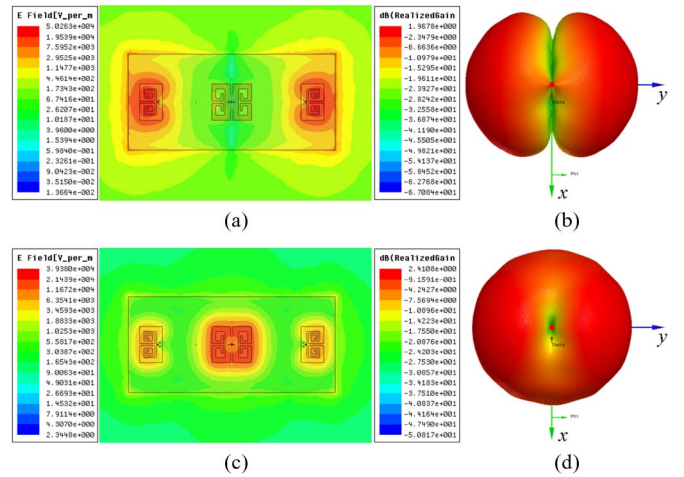
IV. SYSTEM INTEGRATION AND EXPERIMENTAL RESULTS

A prototype of the proposed radio repeater is fabricated using a 3.18-mm-thick Rogers RO-5880 substrate ($\epsilon_r = 2.2$), as shown in Fig. 12. As shown, the top side of the substrate accommodates the TX array and RX antennas. At the backside, a very thin substrate includes the ring hybrid coupler, the RF amplifier, and the dc-bias circuitry. Furthermore, a small



(b)

Fig. 10. Miniaturized radio repeater: (a) geometry of the miniaturized radio repeater and (b) simulated S-parameters.



(a)

(b)

(c)

(d)

Fig. 11. Simulated fields profiles: (a) near E-field distribution (TX mode); (b) E-field radiation pattern in $H(xy)$ plane; (c) near E-field distribution (RX mode); (d) E-field radiation pattern in $H(xy)$ plane.

commercial Lithium-Polymer cell is incorporated at the backside for furnishing power over an extended period of time. To obtain the required gain and output power while maintaining low-power consumption, a cascaded RF amplifier composed of a high-gain (20 dB), low-noise, and low-power amplifier (μ UC8182T made by NEC) and a moderate-power (20 dBm) and high-gain (30 dB) amplifier (μ PG2250T5N made by NEC) are integrated into the system. The total gain of the cascaded RF amplifier can be adjusted by controlling the dc bias voltage. To provide an adjustable dc bias, a power-efficient voltage

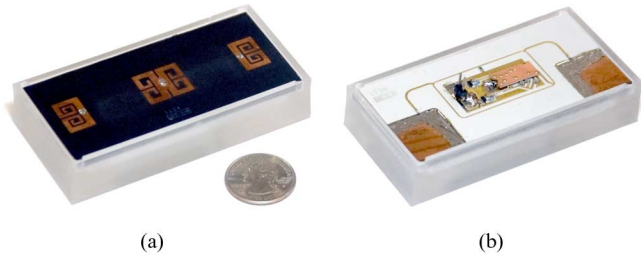


Fig. 12. Prototype of the miniaturized radio repeater: (a) TX array and RX antenna and (b) RF amplifier and modified ring hybrid coupler.

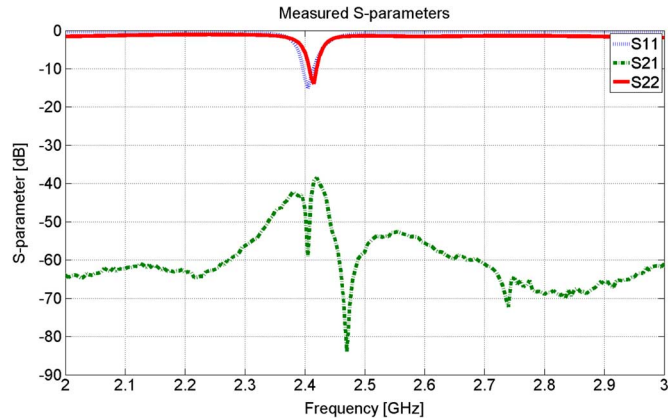


Fig. 13. Measured S-parameters of the miniaturized radio repeater.

regulator (MAX8892 made by MAXIM) is utilized. At a bias voltage of 3 V, the two stages of RF amplifiers are measured to provide 50 dB of gain and draw 80 mA.

As an initial test of the radio repeater system including the ring hybrid coupler, the two-port S-parameters of the antennas are measured by connecting coaxial cables to the RX antenna and the input port of the ring coupler. The measured S-parameters are shown in Fig. 13, where a good input impedance matching for the RX antenna and TX antenna array is observed. A minimum isolation of about 40 dB is also observed. It is noted that this is the worst case scenario as the asymmetric placement of coaxial cables in the near field of the antennas perturbs the symmetry and creates more than expected crosstalk. To avoid such difficulties in the measurement of the mutual coupling, the repeater is characterized in the far field using a radar system in backscatter mode. In this approach, the repeater backscattering RCS is measured with different amplifier gain values while its oscillation is monitored using a spectrum analyzer. No oscillation occurs for the maximum gain value of 50 dB. Fig. 14 shows the repeater in the anechoic chamber of The University of Michigan.

Fig. 15(a) shows the radar outputs as a function of frequency for both the repeater and a 0.36-m-diameter sphere. At the operating frequency (2.43 GHz), the measured repeater RCS is 31.3 dB higher than the sphere, which corresponds to a RCS value of 21.3 dBsm. This value corresponds to the RCS of a 13.1-m-diameter metallic sphere. In addition, the far-field RCS pattern at VV polarization is also measured and shown in Fig. 15(b). As mentioned before, the proposed repeater shows the electric null plane along the symmetric plane and a 3-dB beamwidth of about 80° in the H -plane.

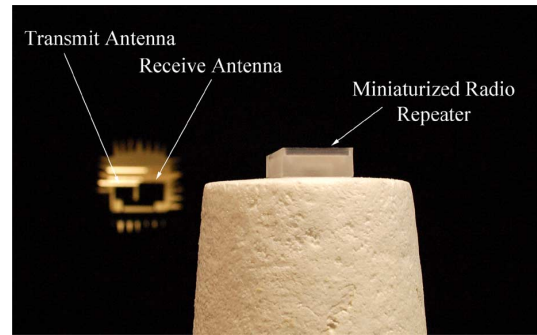


Fig. 14. Monostatic RCS measurement setup.

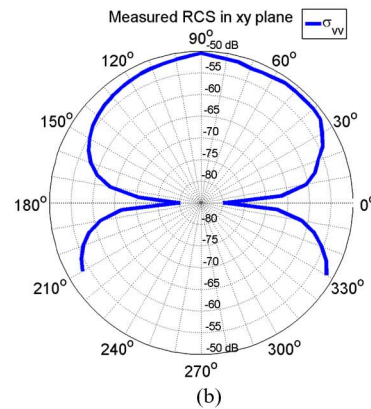
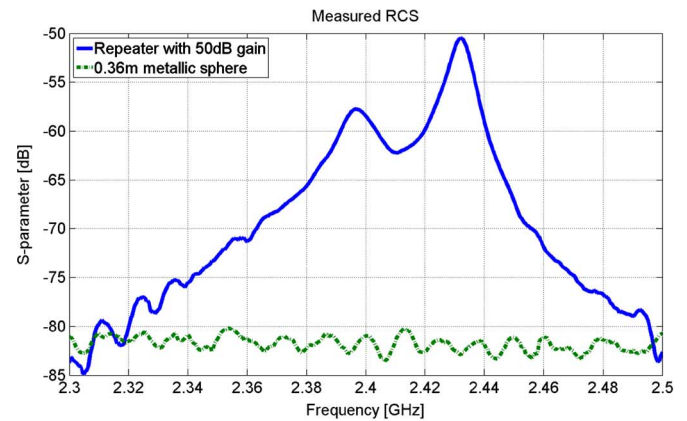


Fig. 15. Measured radar outputs: (a) repeater RCS and (b) repeater RCS pattern in $H(xy)$ plane.

V. CONCLUSION

In this paper, a novel concept for development of a high-gain and miniaturized radio repeater is presented. The repeater system is composed of miniaturized low-profile planar antennas ($\lambda_0/39$) radiating vertical polarization, a modified ring hybrid coupler for feed the TX antenna array, and a low-power high-gain amplifier chain, which are integrated into a compact configuration. The RX antenna is designed to show an omni-directional radiation pattern. The TX array is composed of two elements, which are designed to maximize the directivity of vertical radiation pattern in the end-fire directions and minimize the mutual coupling to the RX antenna. The near-field cancellation is accomplished using the modified ring hybrid coupler, which feeds the TX array with equal amplitude and 180° out of phase to generate a null plane in the middle of the TX array where the

RX antenna is placed. As a result, the proposed radio repeater is shown to suppress the mutual coupling down to -54 dB over the entire frequency band. The proposed radio repeater is fully integrated including a dc bias circuitry and battery. Its dimensions are $85.39 \text{ mm} \times 39.67 \text{ mm} \times 3.48 \text{ mm}$, which corresponds to $\lambda_0/1.45 \times \lambda_0/3.11 \times \lambda_0/35.48$. The proposed radio repeater system has been evaluated and verified both numerically and experimentally.

REFERENCES

- [1] N. Blaunstein and Y. Ben-Shimol, "Prediction of frequency dependence of path loss and link-budget design for various terrestrial communication links," *IEEE Trans. Antennas Propag.*, vol. 52, no. 10, pp. 2719–2729, Oct. 2004.
- [2] Y. Wang, S. Safavi-Naeini, and S. Chaudhuri, "A hybrid technique based on combining ray tracing and FDTD methods for site-specific modeling of indoor radio wave propagation," *IEEE Trans. Antennas Propag.*, vol. 48, no. 5, pp. 743–754, May 2000.
- [3] S. K. Park, P.-J. Song, and G. S. Bae, "Joint optimization of radio repeater location and linking in WLL systems with 2.3 GHz frequency band," in *Proc. IEEE Int. Conf. Commun. (ICC)*, 1999, vol. 3, pp. 1617–1621.
- [4] P. Slobodzin, "Estimation of the repeater gain required for a wireless link," in *Proc. 15th Int. Conf. Microw., Radar, Wireless Commun. (MIKON)*, May 2004, vol. 2, pp. 656–659.
- [5] M. Patwary, P. Rapajic, and I. Oppermann, "Capacity and coverage increase with repeaters in UMTS urban cellular mobile communication environment," *IEEE Trans. Commun.*, vol. 53, no. 10, pp. 1620–1624, Oct. 2005.
- [6] J. Borkowski, J. Niemela, T. Isotalo, P. Lahdekorpi, and J. Lempiainen, "Utilization of an indoor DAS for repeater deployment in WCDMA," in *IEEE 63rd Veh. Technol. Conf. (VTC 2006-Spring)*, May 2006, vol. 3, pp. 1112–1116.
- [7] A. H. Naemat, A. Tee, A. S. M. Marzuki, B. Mohmd, K. Khalil, and A. R. A. Rahim, "Achieving optimum in-building coverage of 3G network in Malaysia," in *Int. RF Microw. Conf. (RFM)*, Sep. 2006, pp. 343–346.
- [8] *Radio Network Planning and Optimisation for UMTS*, J. Laiho and T. N. Achim Wacker, Eds., 2nd ed. New York: Wiley, Feb. 2006 [Online]. Available: <http://dx.doi.org/10.1002/9780470031407.fmatter>, no. 978-0-470-01575-9
- [9] T. W. Ban, B. Y. Cho, W. Choi, and H.-S. Cho, "On the capacity of a DS/CDMA system with automatic on-off switching repeaters," in *IEEE Int. Conf. Commun. (ICC)*, 2001, vol. 3, pp. 780–784.
- [10] M. Lee, B. Keum, Y. Son, J.-W. Kim, and H. S. Lee, "A new low-complex interference cancellation scheme for WCDMA indoor repeaters," in *Proc. IEEE Region 8 Int. Conf. Comput. Technol. Electr. Electron. Eng. (SIBIRCON)*, Jul. 2008, pp. 457–462.
- [11] J.-Y. Choi, M.-S. Hur, Y.-W. Suh, J.-S. Baek, Y.-T. Lee, and J.-S. Seo, "Interference cancellation techniques for digital on-channel repeaters in T-DMB system," *IEEE Trans. Broadcast.*, vol. 57, no. 1, pp. 46–56, Mar. 2011.
- [12] K. Sarabandi and Y. J. Song, "Subwavelength radio repeater system utilizing miniaturized antennas and metamaterial channel isolator," *IEEE Trans. Antennas Propag.*, vol. 59, no. 7, pp. 2683–2690, July 2011.
- [13] J. Oh, M. Thiel, and K. Sarabandi, "Wave propagation management in indoor environments using micro-radio repeater systems," *IEEE Antennas Propag. Mag.*, 2012, accepted for publication.
- [14] D. Liao and K. Sarabandi, "Terminal-to-terminal hybrid full-wave simulation of low-profile, electrically-small, near-ground antennas," *IEEE Trans. Antennas Propag.*, vol. 56, no. 3, pp. 806–814, Mar. 2008.
- [15] D. Sievenpiper, L. Zhang, R. Broas, N. Alexopolous, and E. Yablonovitch, "High-impedance electromagnetic surfaces with a forbidden frequency band," *IEEE Trans. Microw. Theory Tech.*, vol. 47, no. 11, pp. 2059–2074, Nov. 1999.
- [16] F. Yang and Y. Rahmat-Samii, "Microstrip antennas integrated with electromagnetic band-gap (EBG) structures: A low mutual coupling design for array applications," *IEEE Trans. Antennas Propag.*, vol. 51, no. 10, pp. 2936–2946, Oct. 2003.
- [17] A. DiAllo, C. Luxey, P. Le Thuc, R. Staraj, and G. Kossiavass, "Study and reduction of the mutual coupling between two mobile phone pifas operating in the DCS1800 and UMTS bands," *IEEE Trans. Antennas Propag.*, vol. 54, pp. 3063–3074, Nov. 2006.
- [18] K. Buell, H. Mosallaei, and K. Sarabandi, "Metamaterial insulator enabled superdirective array," *IEEE Trans. Antennas Propag.*, vol. 55, no. 4, pp. 1074–1085, Apr. 2007.
- [19] D. M. Pozar, *Microwave Engineering*, B. Zobrist, Ed., 3rd ed. New York: Wiley, 2005.



Young Jun Song (S'07) received the B.S. degree in electrical engineering (*summa cum laude*) from the Seoul National University, Seoul, Korea, in 2006, and the M.S.E. degree in electrical engineering and the M.S. degree in mathematics from The University of Michigan, Ann Arbor, in 2009 and 2012, respectively.

He is currently working towards the Ph.D. degree at The University of Michigan.



Kamal Sarabandi (S'87–M'90–SM'92–F'00) received the B.S. degree in electrical engineering from the Sharif University of Technology, Tehran, Iran, in 1980, the M.S. degree in electrical engineering in 1986 and the M.S. degree in mathematics and the Ph.D. degree in electrical engineering from The University of Michigan at Ann Arbor, in 1989.

He is currently the Director of the Radiation Laboratory and the Rufus S. Teesdale Professor of Engineering in the Department of Electrical Engineering and Computer Science, The University of Michigan, Ann Arbor. His research areas of interest include microwave and millimeter-wave radar remote sensing, metamaterials, electromagnetic wave propagation, and antenna miniaturization. He possesses 25 years of experience with wave propagation in random media, communication channel modeling, microwave sensors, and radar systems and leads a large research group including two research scientists and 14 Ph.D. students. He has graduated 38 Ph.D. and supervised numerous postdoctoral students. He has served as the Principal Investigator on many projects sponsored by the National Aeronautics and Space Administration (NASA), Jet Propulsion Laboratory (JPL), Army Research Office (ARO), Office of Naval Research (ONR), Army Research Laboratory (ARL), National Science Foundation (NSF), Defense Advanced Research Projects Agency (DARPA), and a large number of industries. Currently, he is leading the Center for Microelectronics and Sensors funded by the Army Research Laboratory under the Micro-Autonomous System and Technology (MAST) Collaborative Technology Alliance (CTA) program. He has published many book chapters and more than 185 papers in refereed journals on miniaturized and on-chip antenna, metamaterials, electromagnetic scattering, wireless channel modeling, random media modeling, microwave measurement techniques, radar calibration, inverse scattering problems, and microwave sensors. He has also had more than 442 papers and invited presentations in many national and international conferences and symposia on similar subjects.

Dr. Sarabandi is a member of Commissions F and D of URSI. He was the recipient of the Henry Russel Award from the Regent of The University of Michigan. In 1999, he received a GAAC Distinguished Lecturer Award from the German Federal Ministry for Education, Science, and Technology. He was also a recipient of the 1996 EECSS Department Teaching Excellence Award and a 2004 College of Engineering Research Excellence Award. In 2005, he received the IEEE GRASS Distinguished Achievement Award and the University of Michigan Faculty Recognition Award. He also received the best paper Award at the 2006 Army Science Conference. In 2008 he was awarded a Humboldt Research Award from The Alexander von Humboldt Foundation of Germany and received the best paper award at the IEEE Geoscience and Remote Sensing Symposium. He was also awarded the 2010 Distinguished Faculty Achievement Award from the University of Michigan. The IEEE Board of Directors awarded him the 2011 IEEE Judith A. Resnik Medal. He served as a member of NASA Advisory Council appointed by the NASA Administrator for two consecutive terms from 2006 to 2010. He is serving as a Vice-President of the IEEE Geoscience and Remote Sensing Society (GRASS) and is a member of the Editorial Board of the PROCEEDINGS OF THE IEEE. He was an Associate Editor of the IEEE TRANSACTIONS ON ANTENNAS AND PROPAGATION and the IEEE SENSORS JOURNAL. In the past several years, joint papers presented by his students at a number of international symposia (IEEE APS 1995, 1997, 2000, 2001, 2003, 2005, 2006, 2007; IEEE IGARSS 1999, 2002, 2007; IEEE IMS 2001, USNC URSI 2004, 2005, 2006, 2010, 2011; AMTA 2006; URSI GA 2008) have received best paper awards.